Nanoscale

Anti-soiling performance of high reflective superhydrophobic nanoparticle-textured mirror

Journal:	*Nanoscale*
Manuscript ID	NR-ART-04-2018-003024.R2
Article Type:	Paper
Date Submitted by the Author:	26-Jun-2018
Complete List of Authors:	Jang, Gyoung Gug; Oak Ridge National Laboratory, Bioscience division Smith, D. Barton; Oak Ridge National Laboratory List, Frederick; Oak Ridge National Laboratory, Chemical Sciences Division Lee, Dominic; Oak Ridge National Laboratory, Chemical Sciences Division Ievlev, Anton; Oak Ridge National Laboratory, Center for Nanophase Materials Sciences Collins, Liam; Oak Ridge National Laboratory, Center for Nanophase Materials Science Park, Jaehyeung; Oak Ridge National Laboratory, Polizos, Georgios; Oak Ridge National Laboratory,

Journal Name

ARTICLE

Anti-soiling performance of high reflective superhydrophobic nanoparticle-textured mirror

Received 00th January 20xx,
Accepted 00th January 20xx

DOI: 10.1039/x0xx00000x

www.rsc.org/

Gyoung Gug Jang*[a], D. Barton Smith[a], Frederick Alyious List III,[b] Dominc F. Lee,[c] Anton Ievlev,[d] Liam Collins,[d] Jaehyeung Park,[e] and Georgios Polizos [a]

The anti-soiling (AS) performance of solar mirrors coated with a highly transparent, superhydrophobic nanoparticle-textured coatings has been characterized. The AS coatings were created on the mirror surface by depositing nano-textured silica nanoparticle layers with ~250 nm thickness using a draw-down coating process, followed by fluorination of the nanoparticles in a molecular vapor deposition process. Highly uniform surface features on the AS-coated mirrors (20×30 cm^2, no measurable loss in specular reflectance, and water contact angle >165°) provided outstanding AS performance. A 4× reduction in the rate of dust accumulation as determined by gravimetric measurement of the accumulated dust on coated versus uncoated mirrors was observed. Additional evidence of a significant reduction in soiling rate was determined during measurements of specular reflectance in an outdoor environment test. The adhesion force between a model sand particle and nano-textured coatings having in the range of hydrophobic to superhydrophobic was also studied. A dramatic decrease in adhesive force acting on the particle was observed with increasing surface hydrophobicity. The results align well with observed dust accumulation on the AS coated mirrors. The AS-coated mirror maintains high reflectivity by shedding dust and resisting dust accumulation, providing a potential benefit when applied to mirrors in the solar field of a concentrating solar power generating plant.

1. Introduction

Soiling and dust accumulation on reflective surfaces of solar system contributes to a significant energy loss in power generation,[1-6] due to significant scattering and absorption of the incident solar irradiation in the presence of a dust layer. For photovoltaic modules, accumulated dust leads to lower output power (*e.g.*, the reduction in current and voltage), the local dusting on some panels affects the overall efficiency of voltage output of the module and even cell failure via hot spots.[2,3,6] Concentrated solar power (CSP) electrical energy generation is an efficient, reliable and cost competitive way to convert sunlight to electricity by using reflective surfaces to concentrate a large area of sunlight onto a small area.[1] The high concentration applications are suitable for the arid, desert regions of the world where the solar spectrum is rich and without shades. Coincidentally, these regions have typically suffered from severe dust accumulation which is a major issue for CSP applications. A 5% loss in reflectivity of the mirrors and heliostats for a CSP solar field is potentially more critical than a 5% loss in transmission of a PV module.[5] Therefore, sustaining high reflectivity of the CSP collectors is key to achieving low electricity costs. Furthermore, a reduction of solar field maintenance costs can be achieved through reduced mirror washing cycles.

Transparent superhydrophobic (SH) nano-textured coatings have broad applications including windows, eyeglasses, camera lenses, photovoltaic panels and solar power mirrors. The water repellence and associated self-cleaning performance of SH coatings[6-16] will significantly enhance the reliability and efficiency of the glass window and mirrors, while drastically reducing cleaning and maintenance costs. However, the fabrication of large scale functional nano-texture coating, for example of SH featured high reflective solar mirror, is a huge challenge because the optical performance is associated with well controlled surface roughness at the scale of sub-100 nm.[7,8] Within the engineered scale, the undesirable Rayleigh and Mie scatterings, resulting in opaque mirror and glass, could be minimized. Various common methods such as etching, spray,

[a] *Energy and Transportation Science Division, Oak Ridge National Laboratory (ORNL), Oak Ridge, TN 37831, USA Email: jangg@ornl.gov*
[b] *Materials Science and Technology Division, ORNL*
[c] *Sustainable Electricity Program Office, ORNL*
[d] *Center for Nanophase Materials Science, ORNL*
[e] *Division of Advanced Materials Engineering, Dong-Eui University, Busan 47340, Korea*

Electronic Supplementary Information (ESI) available: See DOI: 10.1039/x0xx00000x

brush, spin coating and dip coating[6-16] have been studied to develop the <100 nm of roughness on glass and mirror surfaces. However, various coating approaches exhibited the intrinsic optical loss (*e.g.,* >5% of transmittance loss).[6,8,10-13] Some approaches showing excellent optical performance with antireflection[14,15] still have challenges such as durability, fabrication cost issues and limitation in the lab-scale substrates, not scalable manner.

The self-cleaning property of SH coatings is often explained when water droplets are dropped on the dusty SH surface, the dust particles stick to the water droplet which then rolls off instead of sliding on the surface and remove effectively the dirt.[6-9] This is due to the low adhesion force of the foreign material to the engineered surface. In this study, we report a scalable SH nanoparticle-textured coating which exhibits outstanding anti-soiling (AS) performance maintaining a clean surface. For the first time, within our best knowledge, we studied the systematic AS property of highly reflective SH nanoparticle-texture coatings on solar reflective mirrors. We also expanded a theoretical adhesion force model describing a model sand particle and the nanoparticle-textured substrates with increasing hydrophobicity to SH properties. The quantified adhesion force on the SH surfaces corresponds with the AS performance of the engineered mirror surfaces. For the scalability, we developed uniform, transparent thin coatings where thin layers of transparent silica nanoparticles bound to the first surface mirror using an inorganic silica sol-gel binder and then post-fluorinated to the coated surfaces. For facile and reproducible nanoparticle self-assembled texture formation, a draw-down coating approach was employed to fit in the roll-to-roll technique for continuous large-scale production. The draw-down coating is a well-known coating technique that was widely used in the coating industry for making liquid thin films in a continuous and controlled manner.[16] The large sized uniform coated mirrors (up to 20×30 cm^2) exhibited excellent AS and optical performance sustaining SH feature (*i.e.,* > 165° of water contact angle) without intrinsic reflectivity loss after coating. Out-door field test revealed the reduction of dust accumulation on the AS coated mirror was achieved, compared with an uncoated mirror.

2. Experimental section

2.1. Preparation of SiO_2 nanoparticle suspension coating solution

Hydrophilic fumed silica nanoparticles (aerosol®380: BET=380 m^2/g) were purchased from Evonik. The SiO_2 nanoparticles (NP) were mixed in ethanol to a concentration of 0.5 wt% and the NP suspension was then sonicated for one hour. After sonication, silica sol-gel was added to the NP solution at a sol-gel/NP weight ratio of 2:1. The coating solution was sonicated for one hour. The sol-gel was synthesized via a modified acidic sol-gel method, as follows. Tetraethoxysilane (TEOS) was dissolved in a mixture of ethanol and deionized water with HCl. The mixture of TEOS: ethanol: H_2O: HCl had a molar ratio of 1:2:2:0.01. After mixing, the Sol was stirred for two hours.

2.2. Preparation of superhydrophobic SiO_2 nanoparticle self-assembly coatings

The application of the coating on solar mirrors was a two-step process. This two-step process was successfully scaled from small mirrors (115 cm^2) to larger mirrors (600 cm^2) during the study. The first step was to deposit a SiO_2 NP self-assembling thin film using a draw-down coater. In a typical first-step for a 20×30 cm^2 second-surface solar mirror, 0.5 mL of the NP coating solution was placed on the glass at the leading edge of the mirror, and a grooved rod (*e.g.,* RDS #3; groove spacing = 0.003 inches) spread the solution at a speed of 2.54 cm/sec using a drawdown machine (Automatic Drawdown Machine, Model DP-8301, GARDCO), leaving a uniform wet film that dried at room temperature [Figure S1 in Supplementary Information]. The spacing of the grooves in the rod dictates the relative thickness of the wet film, which is specified as ~7.6 µm for the RDS #3 rod. The hydroxyl groups on the mirror surface promote uniform wetting of the surface with the hydrophilic SiO_2 NPs solution. A few seconds after the draw-down the wet film was dry, leaving a uniformly thick, transparent thin film. The draw-down coating process was repeated until the desirable thickness was obtained (*e.g.,* application of two layers resulted in a coating with 200~250 nm thickness after drying).

In the second step, the bound SiO_2 NPs were functionalized at the surface via thermal vapor deposition of a fluorosilane solution. The fluorination was carried out with the mirror in a glass-walled chamber and exposed to heated vapor from a (heptadecafluoro-1,1,2,2-tetrahdydrodecyl) trichlorosilane solution (1 wt% fluorosilane in hexane, 30 mL for a 600 cm^2 mirror). The chamber was placed in a furnace and heated to 120 °C for one hour to react the fluorosilane solution with the NPs. After fluorination, the coated mirror was rinsed with H_2O, acetone and isopropanol. The resulting coating was superhydrophobic with water contact angles ≥ 165°.

2.3. Characterization

Scanning electron microscopy (SEM) was carried out using a field emission scanning electron microanalyzer (Merlin, Carl Zeiss AG). Water contact angles (WCA) were measured by an optical tensiometer (OneAttension, Biolin Scientific). Specular reflectances from 330 to 2500 nm spectral band were measured using a portable reflectometer (410-Solar, Surface Optics Corporation). The surface chemistry of a coated sample was characterized using Time-of-Flight Secondary Ion Mass Spectrometry (ToF-SIMS). Dust particle sizes were determined by an optical microscopy. Image analysis of the luminosity of selected areas in photographs taken during the field test was performed to evaluate the effects of moisture on the mirror surfaces. Image analysis was done using the Gel analysis tool in ImageJ (an open source scientific software for image analysis).

2.4. Adhesion force measurements

Using atomic force microscopy (AFM), we measured the adhesion force between synthetic dust particles made of silica (SiO_2: 15 µm diameter) and various nanostructured hydrophobic surfaces. To simulate the adhesion forces in the field, we used AFM cantilevers with a silica sphere attached to the end of the tip. A scanning electron microscopy (SEM) image of the cantilever is shown in supplementary information. The adhesion force on coatings with WCA ranging from 110 to 168° was measured. The topography and

surface functionality of the coatings was controlled by varying sol-gel/NP weight ratio from 2 to 32. As the ratio increased, the WCA decreased from 168° to 110°.

The AFM used for humidity study was a Cypher ES instrument (Asylum Research an Oxford Instr. Company), used in conjunction with a borosilicate colloid probe cantilever (Novascan) of diameter 6 µm and a calibrated spring constant of 4.53 N/m. For humidity control, the inlet for the environmental scanner was supplied with a continuous flow of nitrogen, diverted from a homemade gas humidifier. The gas bubbler/humidifier could be controlled to determine the humidity passing to the cell, which was measured close to the microscope cell by a humidity probe. It was possible to control the humidity in the range 2-80% RH. For each humidity measurement the cell environment was allowed to stabilize for ~30 mins before commencement of the adhesion measurement. For each humidity a total of 625 force curves collected in a grid over 25 µm of each sample. From these measurements the mean and standard deviation adhesion forces were calculated and plotted versus humidity.

2.5. Soiling rate measurement

There is no standardized or wide accepted test for measuring the "soiling rate" on solar mirror,[17,18] so we improvised a gravimetric method for quantifying the mass of accumulated soil on mirror surfaces. This improvised method provided reproducible results for measurements on small area mirrors. A photograph of the test apparatus used for this method is shown in the supplementary information. The apparatus was a Falling Sand Abrasion Tester (ASTM D968, Standard Test Methods for Abrasion Resistance of Organic Coatings by Falling Abrasive) that is modified to provide a uniform areal distribution of standard test dust (ISO 12103-1 A4 Coarse Sand) on a test surface and thereby mimic the natural accumulation of dust on solar mirrors at CSP plants. A prescribed quantity of test dust was introduced at the top of the guide tube (120 cm long, 7.6 cm inside diameter) by dispersing it uniformly across the entire surface of a size 18 mesh (1 mm sieve size) that covered the circular opening of the tube. The mesh provided an initial dispersion of the test dust at the beginning of its descent and the air in the tube further dispersed the dust during its descent. The dust was applied incrementally to slow the rate of accumulation and to minimize the interaction between falling dust particles and dust particles that accumulate on the test surface. The falling dust emerged at the bottom of the tube and collided with the inclined surface of a 3×3 inch^2 mirror under test. The mirror under test was in open air and dust that did not adhere to its surface was able to bounce off or flow away without impedance. The elevations of the inclined mirror surface (all angles measured from the horizontal plane) were 30°, 45° and 60°. After the dust had fallen, the mirror sample was carefully removed from the holder and transferred to a scale while taking care to prevent the loss of adhered dust. The increase in mass of the mirror was a direct indication of the amount of soil that accumulated on the surface. After weighing, measurements of the specular reflectance were made at multiple locations on the soiled mirror using the portable reflectometer.

3. Results and Discussion

3.1. Coating characteristics on large mirrors

A large area, solar specular reflectance loss-free SiO_2 NP self-assembly thin layer was deposited by a rod draw-down coating. AS coatings were applied to 600 cm^2 solar mirrors using the draw-down method and post functionalization. Figure 1a shows one of the mirrors after a two-layer application of SiO_2 NPs with the silicate sol-gel binder followed by functionalization of the NPs by vapor phase fluorination. The two-layer coatings had a typical thickness of ~250 nm and a uniform surface texture with 30.1 nm of RMS roughness [Figure 1b&c, Supplementary Information]. Before being coated, the mirrors have a WCA ~40°. After coating and before fluorination, the NP-textured surfaces were highly hydrophilic with WCA ≤ 5°, a condition attributable to the presence of hydroxyl groups on the rough surface. After fluorination, the textured coatings were superhydrophobic with WCA > 165°.The chlorosilane groups present in the fluorosilane were hydrolysed during the thermal treatment and hydrogen-bonded to the surface of the silica NP. The depth profile of ToF-SIMS revealed that a strong fluorine (Cs_2F^+) signal was present at the AS coated surface, but not at the surface of uncoated glass [Figure 2a]. The SH NP-textured coating, in other word AS coating, was studied for characterization and anti-soiling performance.

To evaluate the optical uniformity of the specular reflectance of the coated mirror, 20 points were selected for measurement. It was necessary to cut the mirror into nine smaller pieces to fit them into the tensiometer for the WCA measurements. Figure 2b shows the average specular reflectances at seven wavelength bands extending from 335 to 2500 nm on AS coated and uncoated (reference) mirrors at a single measurement location for each mirror. The reflectances of the AS coated mirror are slightly higher than the uncoated mirror at each of the wavelength band. The average specular reflectance measured on the AS coating (0.924 ± 0.006, n=20) in Figure 2c is statistically indistinguishable from the average reflectance measured on the uncoated mirror (0.921 ± 0.006, n=20). These measurements show that the SiO_2 NP AS coating can be applied to solar mirrors without concern that they will negatively impact their characteristic specular reflectance. The transparency of the coating is a critical performance parameter for maintaining the reflectance of CSP mirrors. A small decrease in the reflection of sunlight due to the presence of the AS coating would have significant impact on overall system performance and viability. To evaluate the uniformity of the superhydrophobicity of the AS coating, measurements of WCA were made at 50 separate points across the coated area of one of the mirrors prepared for a field evaluation. Figure 2d illustrates the very small standard deviation in the WCA (distributed mostly from 162.1° to 168.5°), indicating that the AS coating was consistently uniform across the entire surface area. The WCAs were measured in the water droplet volume range from 5.7 µl to 10.6 µl, where WCAs were less dependent on the volume [Supplementary Information]. The uncoated mirror is hydrophilic with an average WCA of 52.6 ± 19.0° (n=30).

3.2. Adhesion force model for the superhydrophobic surfaces

The surface structure of the AS coatings (*i.e.,* SH NP-textured coatings) provides an intrinsic capability for repelling small dust particles. To predict the anti-soiling effectiveness of the AS coatings

as a function of hydrophobicity, the magnitude of the adhesion force between a dust particle and the surface was measured and correlated to the observed soiling and degree of hydrophobicity. The measured and analytically predicted adhesion forces are summarized in Figure 3. The predicted values are based on the van der Waals attraction between particle and surface. These values were calculated according to equation 1.[19]

$$F_{vdW} = \frac{AD}{12a^2}\left[\frac{1}{1+\left(\frac{16Dk_1rms}{\lambda^2}\right)} + \frac{1}{1+\left(\frac{k_1rms}{a}\right)^2}\right] \quad (1)$$

In the above equation, a is the distance between the particle and the surface (which is 0.3 nm, when the particle is in contact with the surface); D is the particle diameter (15 μm); *rms* is the root mean square surface roughness; k_1 is a constant (1.817); λ is the distance between the asperities; and A is the Hamaker constant. The Hamaker constant was calculated according to the mixing rule for dissimilar surfaces $\boldsymbol{A = \sqrt{A_1 A_2}}$, where A_1 is the Hamaker constant for the fused silica (6.6×10^{-20} J) and A_2 is the Hamaker constant for the fluorine compound, poly(tetrafluoroethylene) (3.8×10^{-20} J). The good agreement between the measured and the predicted values indicates that the van der Waals contribution is the dominant component for the adhesion force between the dust particles and the coated substrate. According to Figure 3, the adhesion force on the AS coating is 4 to 5 times smaller than the adhesion force on the non-structured substrate (i.e., fluorinated on bare Si wafer). According to equation 1, the adhesion force depends strongly on the surface roughness (*rms* and λ values). The WCA values on SH surfaces are increasing when the surface roughness is increasing. The WCA is inherently associated with the surface roughness factor, r, and is scaled according to the modified Young's equation, $r=\cos\theta_{SH}/\cos\theta_0$. The theoretical prediction for the variation of the van der Waals force for different surface structures is shown in Figure 3. Based on these dependencies, it is possible to further decrease the adhesion force by optimizing the *rms* and λ values.

Figure 4 shows the adhesion force of another model particle (6 μm) on AS coated and uncoated mirror surfaces as a function of relative humidity (RH). The adhesion force on the AS coated mirror was >10 times lower than the uncoated surface at 2~80% of RH. This behaviour is well matched with the developed modelling. The adhesion force of the particle on the uncoated mirror surface increases with increasing RH. It could be explained that adsorbed water molecules on the hydrophilic surface form a meniscus between the particle and the surface at high RH, resulting in increased adhesion force.[20] However, the adhesion force of the particle on the AS coated surface was not influenced by RH. This behaviour is attributed to the superhydrophobic surface (WCA= ~165°) associated with roughness and low surface energy coating, resulting in very low adsorption of water molecules at high RH. It was reported that hydrophobic surface is less influenced by RH, because the meniscus formation between the particle and hydrophobic surface occurs at the high RH.[20] For example, the RH level for meniscus formation for a gold surface (WCA=80°) was calculated to 60-65 % of RH.

3.3. Lab-based soiling rate measurement of AS coated mirrors

The AS coated mirrors demonstrated an excellent dust-repellent capability in tests conducted in our laboratory. Figure 5 shows magnified optical images of soiling features when 1g of dust was dispersed on the surface of coated and uncoated mirrors (=220 g/m^2) using the falling sand apparatus with the mirrors inclined at an elevation of 45°. The soiling on the AS coated surface is primarily sparsely distributed agglomerates of dust particles (few mm sized) [Figure 5a], while large agglomerates and individual particles (< 5μm) are densely distributed on the surface of the uncoated mirror [Figure 5b]. The optical microscopy was focused on the particles at the surface. The image of large sized agglomerates was blurred due to out-of-focus. Note that the absence of small dust particles was observed on the AS coating. To simulate mild surface cleaning provided by naturally occurring winds, the soiled surfaces were gently air brushed with a squeezed-bulb dust blower (air volume ~40 mL per puff). The air brushing removed dust adhered by gravity but was insufficiently powerful to remove dust that was electrostatically adhered. The large dust agglomerates on both the coated and uncoated mirrors were effectively removed by the air brushing. Most notably, the small amount of air brushing was able to remove most of the smaller dust particles from the AS coated surface, leaving a few of the finer particles (< 1μm) on the surface [Figure 5c]. The smaller dust particles (<5 μm) were too strongly adhered to the uncoated mirror surface to be removed by air brushing [Figure 5d]. Particle size distribution charts shown in the insets of Figures 5c and 5d show the distributions of particles after air brushing. The particle distribution for the AS coated surface was narrow and centered at 1.19 ±0.34 μm (n=24 from 8977 μm^2 of image analysis area), compared to the distribution for the uncoated surface, which was broad and centered at 2.03 ±1.49 μm (n=375 from the same size area) of dust particles. The dust distributed on the AS surface covered 0.3% of the area used for the analysis corresponded to 0.929 of reflectance, while the 20.8 % of uncoated surfaces covered with dust corresponds to 0.520 of reflectance. The optical image shown in the inset of Figure 5c is the AS coating magnified 5000×. The surface features are representative of those on the entire coating. We believe this NP-texturing at the sub-micrometer-scale is the key to the AS property of the coating. The texturing is an engineered surface roughness that influences the large reduction in the adhesion force. During dust accumulation on an uncoated mirror, the dust particles arrive at the surface via gravity and are then attracted to the surface by electrostatic charges.[18] After settling, particles are held on the surface by van der Waals, a charge double-layer, surface energy, and capillary forces, in addition to the gravitational and electrostatic forces on the mirror surfaces.[19,21] Theoretically, the adhesion force should decrease with particle size. In practice, however, a dry-cleaning technique such as removing particles with a gas jet (usually air or nitrogen) is not effective for particles smaller than 10 μm.[22] There are two physical issues[23]; 1) the force applied to a particle from a fluid flow is proportional to its cross-sectional area, so the removal force decreases faster than the adhesion force as the size decreases, and 2) the velocity of laminar air flowing over surface decreases to zero at the surface. So, for a given air velocity, smaller (shorter) particles reside in a slower air flow than do larger (taller) ones. Turbulence does not contribute to particle removal, because turbulent flow does not extend to the surface; a small but significant region of laminar flow remains near the surface. We found that the

removal of the accumulated dust on uncoated mirrors was possible only by brushing the surface while rinsing it with water.

Comparisons of the soiling rates for AS coated mirrors and uncoated mirrors are shown in Figure 6. Gravimetric measurements of the soiling rates were carried out with both mirrors inclined at elevations of 60°, 45° and 30° to allow the effect of gravity to progressively retard the accumulation of dust and to mimic the range of mirror elevations on CSP heliostats. The applied dust was increased in increasements to an amount we estimated would be the annual fall in Arizona desert in the southwestern United States (*i.e.,* ~909 g/m^2).[22] After measuring the mass of dust that accumulated during the falling dust experiment, we air brushed the mirrors *in situ* and re-measured the mass of the residual dust. Figure 6a shows that the initial accumulations for the AS coated and uncoated mirrors were approximately equal at 30° elevation. As more dust was applied, the quantity of accumulated dust increased linearly for both mirrors. At this elevation the gravitational force dominates the mechanisms by which dust accumulates. The AS performance of the coated mirror was dramatically apparent after the large dust particles and agglomerates were removed with gentle air brushing. Nearly all the dust was removed from the AS coated surface, resulting in a clean surface, while the uncoated surface was still covered with fine dust particles [inset of Figure 6b]. The residual dust amount on the uncoated mirror was about 4 times larger than that on the coated mirror. Figure 6c shows that at a mirror elevation of 45° the AS-coated mirror had very little accumulation as the amount of applied dust increased, while the uncoated mirror had a nearly linear increase in dust accumulation. The accumulation rate of the uncoated mirror was reduced by about 50% when compared that measured at 30° elevation. After removal of the large dust particles with air brushing, the quantity of residual dust on the uncoated mirror was approximately 5 times larger than that of the AS coated mirror [Figure 6d]. Figure 6e shows that at 60° elevation the accumulation rate on the uncoated mirror was dramatically reduced but small dust particles continued to accumulate across the entire surface. On AS coated mirror, most of the applied dust slid off the surface and the accumulated dust was sparse [inset of Figure 6e]. Interestingly, the residual dust on the uncoated mirror after air-brushing was 9 times greater than the residual dust remaining on the AS coated mirror. The increasing amount of residual dust on the uncoated mirror as elevation increased could be attributable to the initial removal of all but the smallest particles by the force of sliding dust. The smaller particles were more likely to adhere by electrostatic charging as the elevation steepened, and the air brushing was characteristically less effective at removing them. The residual dust accumulation rate for uncoated mirror increased with elevation while the dust accumulation rate on AS coated mirror was statistically insignificant at all three elevations.

After the application of dust by the falling sand apparatus, mirror samples with the AS coating had exceptionally good recovery of their specular reflectance when we removed loosely adhered dust by simulating the natural action of wind by air brushing. Figure 7 shows the specular reflectances of coated and uncoated mirrors that were measured after air brushing. For each of the three elevations tested (30°, 45°, 60°), mirrors with the AS coating maintained their specular reflectance. Dust was visibly apparent on the surface of the mirrors but its presence did not yield a decrease in reflectance. On the other hand, the uncoated mirrors experienced significant decreases in reflectance at all three elevations. The decreases were most dramatic as the areal density of applied soil reached a value of 100 g/m^2. At this density the reflectances decreased 25, 30 and 40% for elevations of 30, 45 and 60°, respectively. The observation that the uncoated mirrors retained more dust the elevation increased was counterintuitive but consistent with the results observed in the gravimetric analysis where the dust accumulation also increased with elevation.

The AS coated mirror exhibited a good durability against the abrasive effect of falling sand and the aging effect of a long-term exposure to UV light. Figure S6a in Supplementary Information shows that the AS coated mirror maintained its superhydrophobicity (WCA = 165.7± 2.1°) after simulating the impact of 15 years of sand falling on the coating. Also, exposure in the lab to intense UV light from a high-pressure Hg lamp showed that the SH functionality (WCA=160.8 ± 2.8°) remained over 2000 hrs [Supplementary Information].

3.4. Field evaluation of AS coated mirrors

A field examination of environmental soiling on AS coated and uncoated mirrors was carried out for 61 days on a sloping roof (18° elevation) at Oak Ridge National Laboratory during the late summer and early fall seasons. The soiling conditions in Oak Ridge, Tennessee, USA (*e.g.,* high humidity, high concentrations of pollen and organic aerosols produced by the surrounding forest, frequent rain) are much different from those in the dry or semi-arid desert environments where CSP plants are sited. For example, CSP mirrors experienced a decrease in reflectance of ~40% during a 15-day period in the dry season in the arid environment at the Tantan site in southwest Morocco[1] whereas only a small decrease in reflectance in the uncoated mirrors was observed during our field examination. (*i.e.,* 5~8% reflectance reduction). Some reduction in daily soiling was alleviated by natural cleaning provided by rain, heavy morning dew and frost formation during the field test period [Figure 8, 9 and 10]. The water repellent nature of the AS coated mirror curtailed the formation of heavy dews, wetting and frosting. Figure 9 compared the selected image contrast ratio of the subject (assigned to [1] in Figure 8) to the background (assigned to [2]) in AS coated and uncoated mirrors for each weather condition. On a sunny day both mirrors had a high contrast ratio (>30), consistent with the accompanying observation of high reflectance. However, at wet conditions (*e.g.,* dew, rain and frost), the uncoated mirror had a significantly lower contrast ratio, a result of the scattering and absorption of light by water droplets and the opaque frosts on the surfaces. The less-wetted AS coated mirror surfaces exhibited distinguishable high contrast ratio, compared with the uncoated mirror surfaces.

Measurements of the specular reflectances across the full solar spectrum showed that the daily degradation of reflectance on the AS coated mirror from soiling was quantitatively less than the daily degradation of the uncoated mirrors [Figure 10]. The average reflectance of the AS coated surface (N=6) was 2 to 3% larger than that of the uncoated mirror over a period of 7 days exposure to the environment. The standard deviation in the average value of the

reflectance of the AS coated mirror was significantly smaller than the deviation in the average reflectance of the uncoated mirror. Because the AS coatings was uniform on the entire surface of mirror, the entire mirror had an AS benefit. The uncoated mirror, in contrast, had non-uniform hydrophilic surface properties (WCA between 28° and 88°) and there was scattered areas of heavy agglomeration of dust particles. Magnified optical images of the mirror surfaces, as shown in Figure 10b and c, reveal that the AS coated surface had a relatively clean surface with a few dust particles, while the uncoated mirror had soiling by accumulation of many fibers and dust particles after 61 days. The AS coated mirror still exhibited an average WCA of 154.6 ± 7.1° (n=10), while the uncoated mirror had an average WCA of 19.4 ± 3.8° (n=10). The accumulated dust produced some hydrophilic behavior on both mirrors. We expected that a possible dust fouling mechanism manifested as loss in reflectance might be induced by a dust-moisture cementation process.[18] Atmospheric dust contains a distribution of inorganic and organic particulates (*e.g.,* pollen) that contain some water soluble and insoluble salts. At high humidity, water-soluble dust particles on the surface form microscopic droplets of salt solutions that also retain any insoluble particles. When dried, the precipitated salt acts as a cement to anchor insoluble particles to the surface. This is a possible explanation for the presence of some dust particles adhered to both the AS and uncoated mirrors.

An accelerated UV aging test was conducted on AS coated and uncoated mirrors in an EMMAQUA (Equatorial Mount with Mirrors for Acceleration) device (Atlas Material Testing Technology, Phoenix, Arizona, USA). Concentrated UV light (295-385 nm) accelerated the UV dose rate such that a 365-day UV dose (360 MJ/m^2) was administered to mirrors under test during a 104-day exposure in the Arizona desert. Each of three mirror samples was 15.2 cm × 7.6 cm in size, with approximately half of each mirror coated and half uncoated. After aging was completed, both mirrors exhibited some hard water deposits left by dried precipitation during wintertime test. The average WCA of AS mirror decreased to 120.0 ± 14.9° (n=10). The accelerated UV exposure and environmental exposure to dust, organics and precipitation decreased the surface hydrophobicity. The uncharacteristically large standard deviation in the WCA can be attributed to the hydrophilic nature of the areas with water deposits. The hard water mark area did not affect significant reflectance reduction, however. The average specular reflectance of the AS coated mirrors was 0.924 ± 0.012 (n= 18), compared with an average of 0.905 ± 0.024 (n= 18) on the uncoated mirrors. We then measured soiling rates on the UV aged mirrors at an elevation of 45° using the previously described lab-based falling dust experiment followed with air brushing. The results of these measurements are graphed in Figure 11. Note that the specular reflectance of the weathered AS coated mirrors maintained their initial reflectance. The weathered uncoated mirrors again exhibited large reductions in reflectance as the area density of incident dust increased. The durability of an AS coating is an important consideration for its use on CSP mirrors. We expect to perform additional, more extensive in-depth characterization of dust-cementation and study environmental fouling mechanisms on AS coated mirrors in future work.

4. Conclusions

The results of our testing on a superhydrophobic nanoparticle-textured coating demonstrate that such a coating had an exceptional anti-soiling performance. The coating is transparent and does not degrade the specular reflectance of the mirrors by its presence. The coating application process used in our lab is scalable to very large areas in a commercial process. The correlation of the adhesion force between a model sand particle and the nano-textured surface of the AS coating provides evidence that the adhesion force decreases as the superhydrophobic character of the surface increases. The decreased adhesive force is the phenomenon that provides an intrinsic soil and dust repellency. Simulations of naturally occurring cleaning agents such as wind and precipitation showed that AS coated mirrors were able to maintain very clean surfaces during lab-based indoor testing as well as during evaluations outdoors in the field. The anti-soiling coating is of tremendous potential benefit to operators of CSP plants by increasing average reflectance of the solar field and reducing the need for mirror washing.

Conflicts of interest

There are no conflicts to declare

Acknowledgements

This research was conducted at the Oak Ridge National Laboratory, which is managed by UT Battelle, LLC, for the U.S. Department of Energy (DOE) under contract DE-AC05-00OR22725. The work was sponsored by the Solar Energy Technologies Office (SETO) within the DOE Office of Energy Efficiency and Renewable Energy (EERE). Some of the materials characterization (including ToF-SIMS, SEM and AFM humidity measurement) was conducted at the Center for Nanophase Materials Sciences, which is sponsored by the ORNL Scientific User Facilities Division and the DOE Office of Basic Research Sciences.

References

1. S. Bouaddi, A. Ihlal and A. Fernandez-García, *Renewable Energy,* 2017, **101**, 437-449.
2. M.R. Maghami, H. Hizam, C. Gomes, M.A. Radzi, M.I. Rezadad, and S. Hajighorbani, *Renewable and Sustainable Energy Reviews,* 2016, **59**, 1307–1316.
3. M. Abderrezek, Mohamed Fathi, Experimental study of the dust effect on photovoltaic panels' energy yield, *Solar Energy,* 2017, **142**, 308–320.
4. M. Saidan, A.G. Albaali, E. Alasis and J.K. Kaldellis, *Renewable Energy,* 2016, **92**, 499-505.
5. M.J. Adinoyi and S.A.M. Said, *Renewable Energy*, 2013, **60**, 633-636.
6. Q. Xu, Z. Zhao, X. Zhu, L. Cheng, S. Bai, Z. Wang, L. Meng and Y. Qin, *Nanoscale*, 2016, **8**, 17747
7. Y. Si and Z. Guo, *Nanoscale*, 2015, **7**, 5922
8. J.T. Simpson, S.R. Hunter and T. Aytug, *Rep. Prog. Phys.*, 2015, **78**, 086501 (14pp).
9. Y. Li, Z. Zhang, M. Wang, X. Men and Q. Xue, *J. Mater. Chem. A,* 2017, **5**, 20277-20288.
10. G. Prasad, R.P.S. Chakradhar, Parthasarathi Bera, A. Anand Parbu and C. Annadan, *Surf. Interface Anal.* 2017, **49**, 427-433.

11. D. Helmer, N. Keller, F. Kotz, F. Stolz, C. Greiner, T.M. Nargang, K. Sachsenheimer and B.E. Rapp, *Scientific Reports*, 2017, **7**, 15078.
12. I.S. Bayer, *Coatings*, 2017, **7,** 12.
13. J.E. Mates, R. Ibrahim, A. Vera, S. Guggenheim, J. Qin, D. Calewart, D.E. Waldroup and C.M. Megaridis, *Green Chem.,* 2016, **18**, 2185-2192.
14. L. Yao and J. He, *Progress in Materials Science* 2014, **61**, 94-143.
15. U. Mehmood, F.A. Al-sulaiman, B.S. Yilbas, B. Salhi, S.H.A. Ahmed and M.K. Hossain, *Solar Energy Materials & Solar Cells*, 2016, **157**, 604-623.
16. J. Wang, M. Liang, Y. Fang, T. Qiu, J. Zhang and L. Zhi, *Adv. Mater.,* 2012, **24**, 2874-2878.
17. T. Lorenz, E. Klimm and K-A. Weiss, *Energy Procedia*, 2014, **48**, 749-756.
18. K. Brown, T. Narum and N. Jing, *Photovoltaic Specialist Conference (PVSC) 2012 IEEE 38th*, pp.001881-001885.
19. Y.I. Rabinovich, J.J. Adler, A. Ata, R.K. Singh and B.M. Moudgil, *J. Colloid Interface Sci.* 2000, **232**, 10-16.
20. H. Kweon, S. Yiacoumi and C. Tsouris, *Langmuir*, 2011, **27**, 14975-14981.
21. T. Sarver, A. Al-Qaraghuli and L.L. Kazmerski, *Renewable and Sustainable Energy Reviews,* 2013, **22**, 698-733.
22. M.A. Felicetti, G.R. Salazar-Banda, J.R. Coury, M.L. Aguiar, *Ind. Eng. Chem. Res.* 2009, **48**, 877-887.
23. Steven Abbortt, Adhesion Science; Principle and Practice, DEStech Publications, Inc. 2015.
24. G. Polizos, G.G. Jang, D.B. Smith, F.A. List, M.G. Lassiter, J. Park and P.G. Datskos, *Solar Energy Materials and Solar Cells*, 2017, **176,** 405-410.

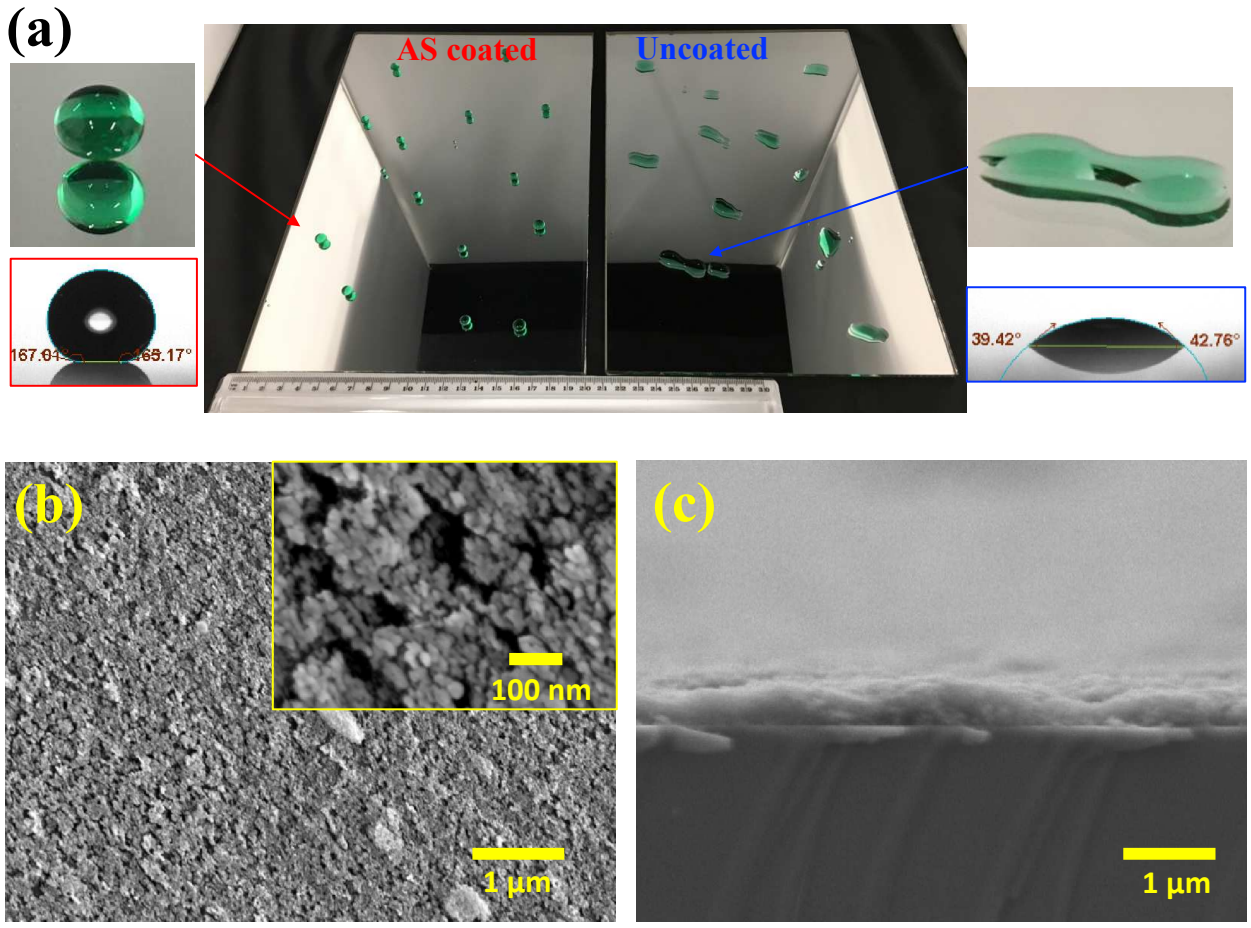

Figure 1 a) A 20×30 cm^2 solar mirror with superhydrophobic anti-soiling coating with nano-textured surface. Insets are water droplets on an AS coated mirror (the measured water droplet volume = 9.6 µl) and an uncoated mirror (the volume = 8.2 µl). b) SEM image of mirror surface, showing characteristics of nano-texturing c) SEM cross-sectional view of AS coating.

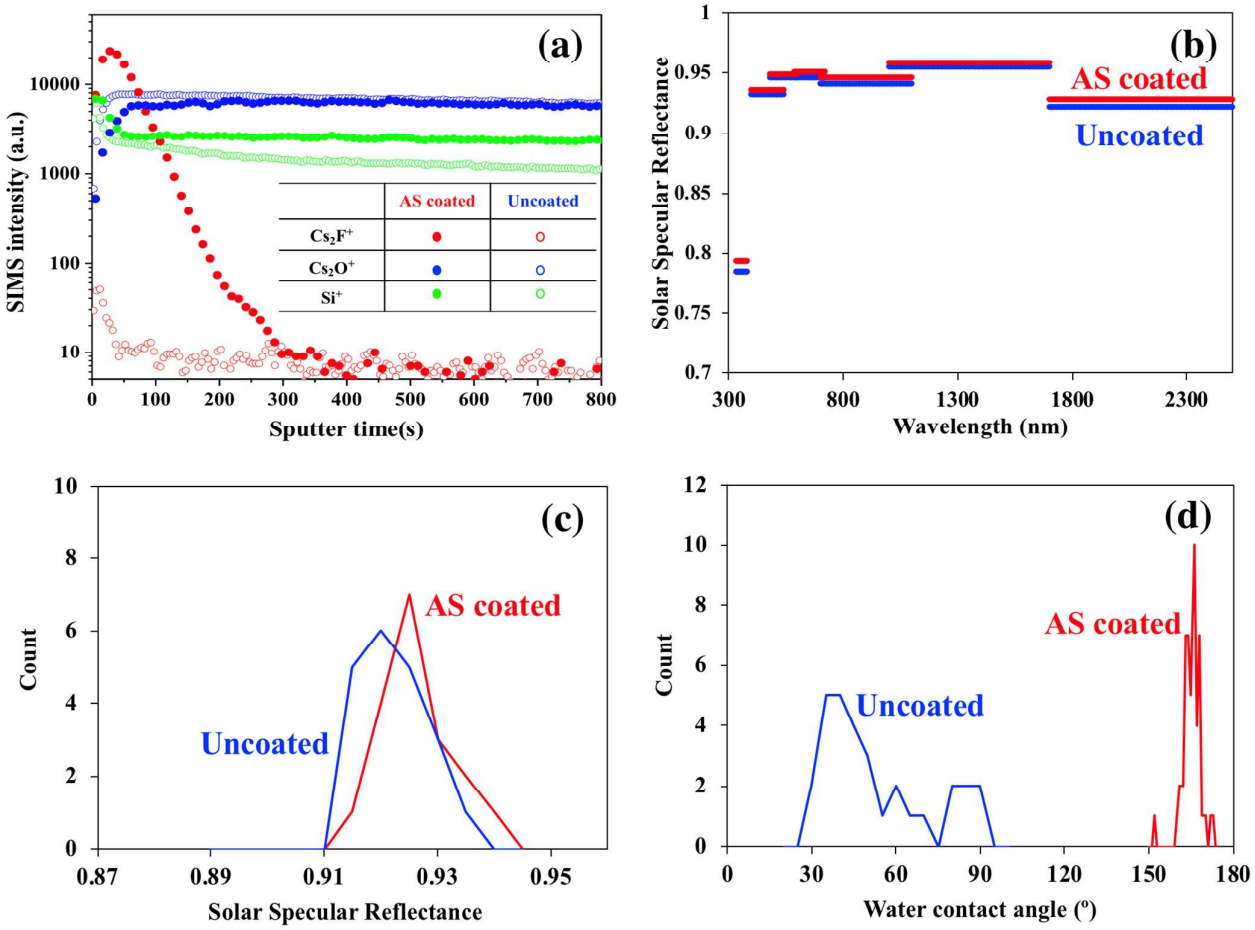

Figure 2 Characterization of AS coating on 20×30 cm^2 solar mirror via compositional analysis, optical reflectance and water contact angle, a) Chemical composition of coating determined by depth profiling of ToF SIMS for three components (F, O, Si), b) Specular reflectances measured in wavelength bands across solar spectrum for AS coated and uncoated mirrors, c) Distribution of specular reflectances measured on AS coated and uncoated mirrors (n=20), d) Distribution of water contact angles measured on coated and uncoated mirrors (n=50). The average values of water droplet volumes on coated and uncoated mirrors are 8.9 ± 1.0 µl (n=50) and 7.1 ± 2.8 µl (n=30), respectively.

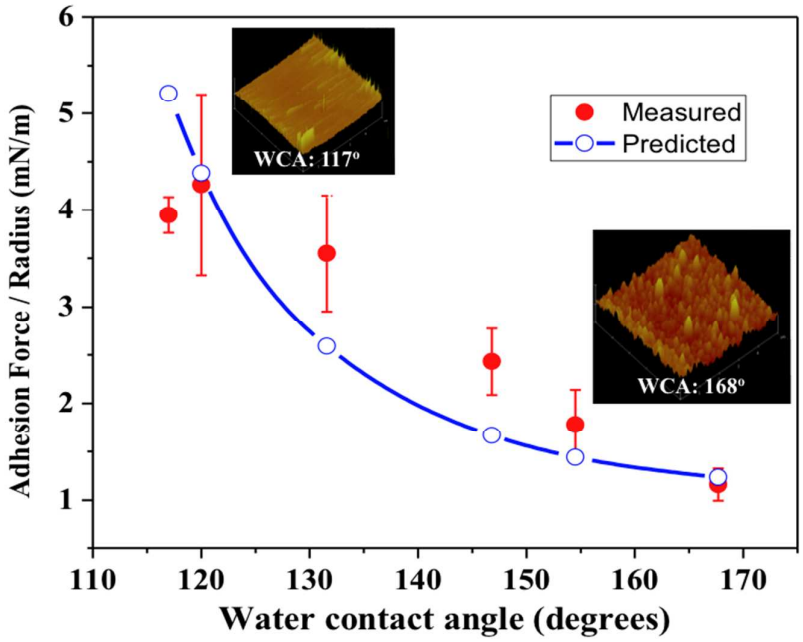

Figure 3 Figure of merit for the adhesion force between 15-μm-diameter spherical dust particle and coated substrates with WCAs in the range 117 to 167.5°. Insets show AFM images of coating surface topography for coatings having WCAs of 117° and 167.5°. The number of force measurements per data point was ≥ 3. Error bars are the standard deviations in the mean values.

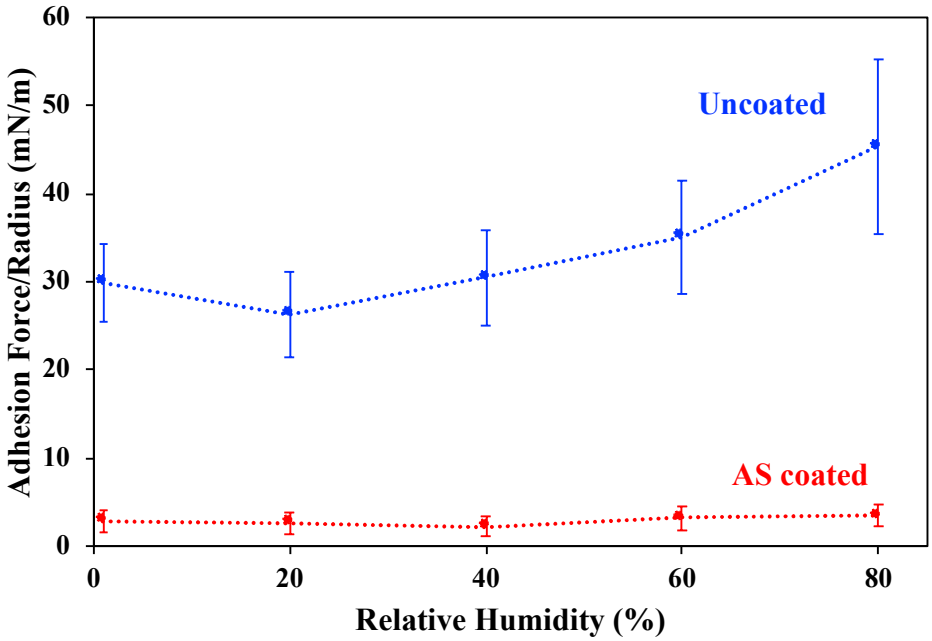

Figure 4 Measurement of adhesion forces between 6-μm-diameter spherical dust particle and AS coated solar mirror and uncoated mirror as a function of relative humidity.

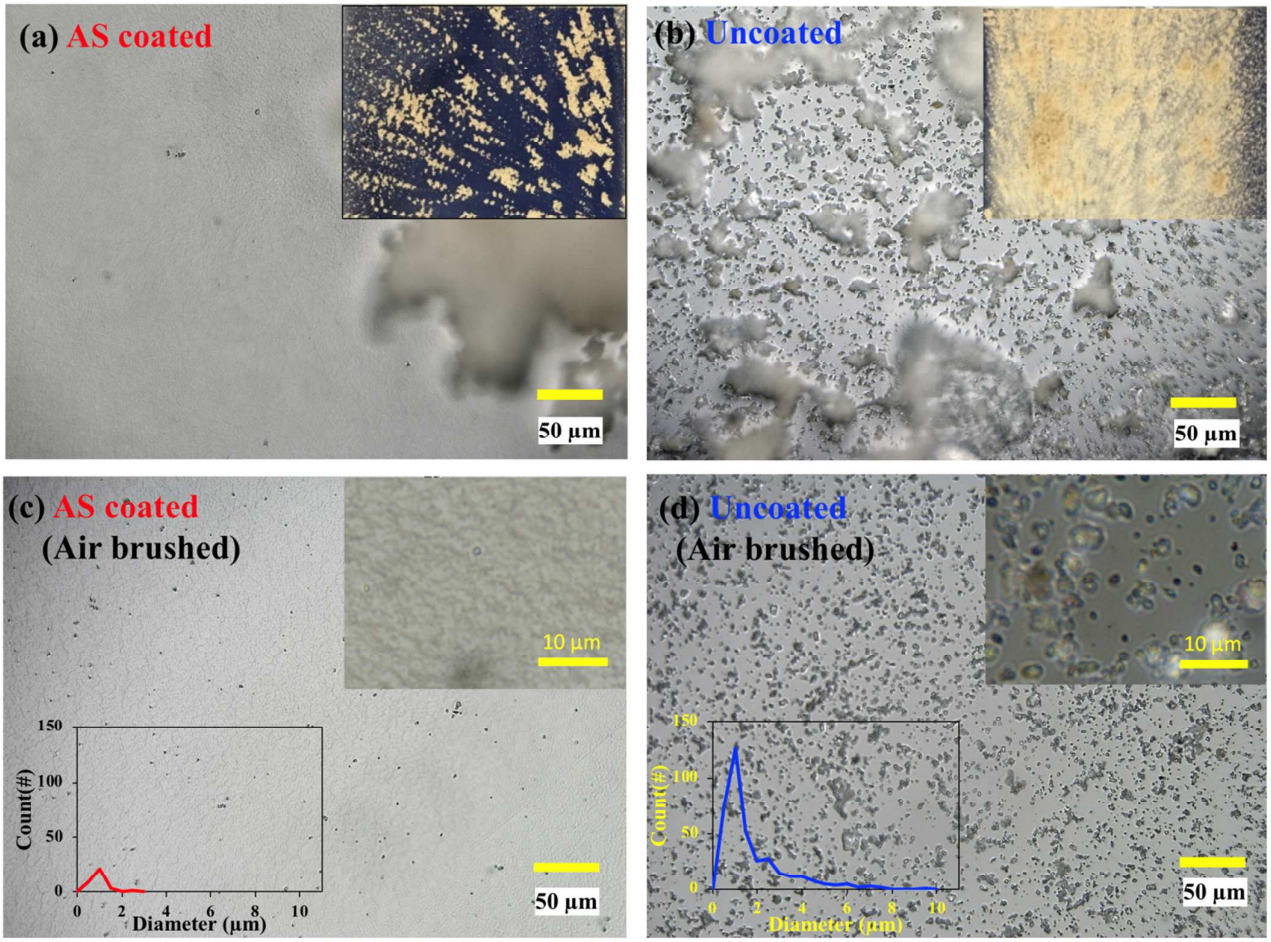

Figure 5 Optical microscope images of soiling on an AS coated mirror and an uncoated mirror. a) Initial soiling on the AS coated surface (×500 magnification, focused on plane of glass surface), Inset is low-magnification photographic image of soiling on the AS mirror, b) Initial soiling on the uncoated surface (×500, focused on plane of glass surface). Inset is low-magnification of photographic image of soiling on the uncoated mirror, c) the AS coated mirror surface after air-brushing (×500). Right upper inset is ×5000 magnificence of the AS surfaces. Inset in lower left is dust particle size distribution obtained by analysis of the images at ×5000 magnification, d) the surface of the uncoated mirror after air-brushing (×500). Right upper inset is ×5000 magnification. Inset in lower left is dust particle size distribution from the images at ×5000 magnification.

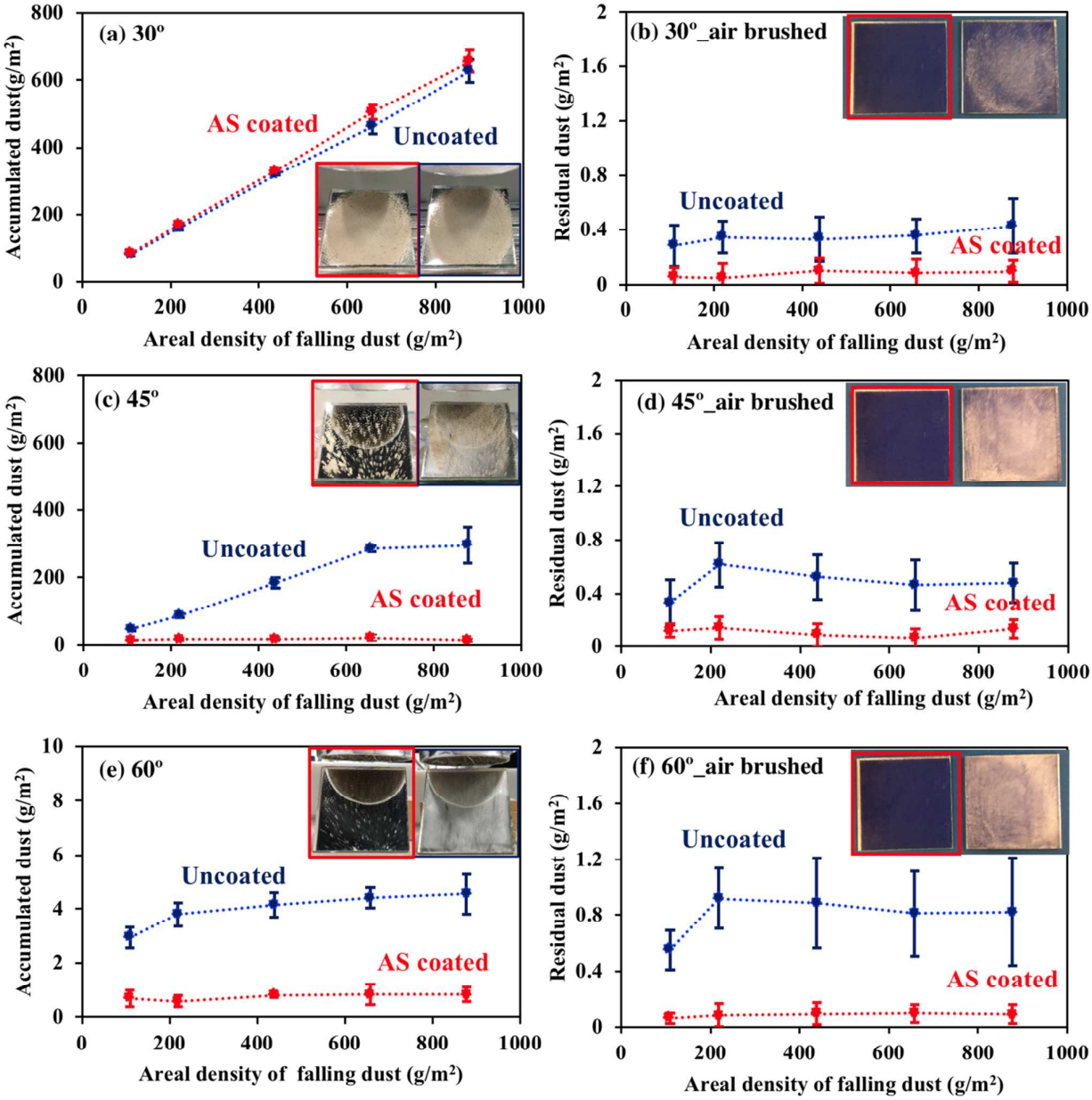

Figure 6 Gravimetric analysis of soiling and dusting effects on an AS coated mirror, compared with the effect on an uncoated mirror, determined as a function of elevation and applied dust. The quantities of accumulated dust were determined using gravimetric analysis after soiling and after air brushing, respectively. a, c, e) Measurement of accumulated dust at 30, 45, 60° elevation, b, d, f) Measurement of residual dust at 30, 45, 60°. Insets are photographic images of each mirrors after application of 1 g of falling dust. The box outlined in red is the AS coated mirror. The number of measurements per data point was ≥ 5, and the error bars are the standard deviations in mean values. Lines are drawn for illustration and are not modelled curve fits to the data.

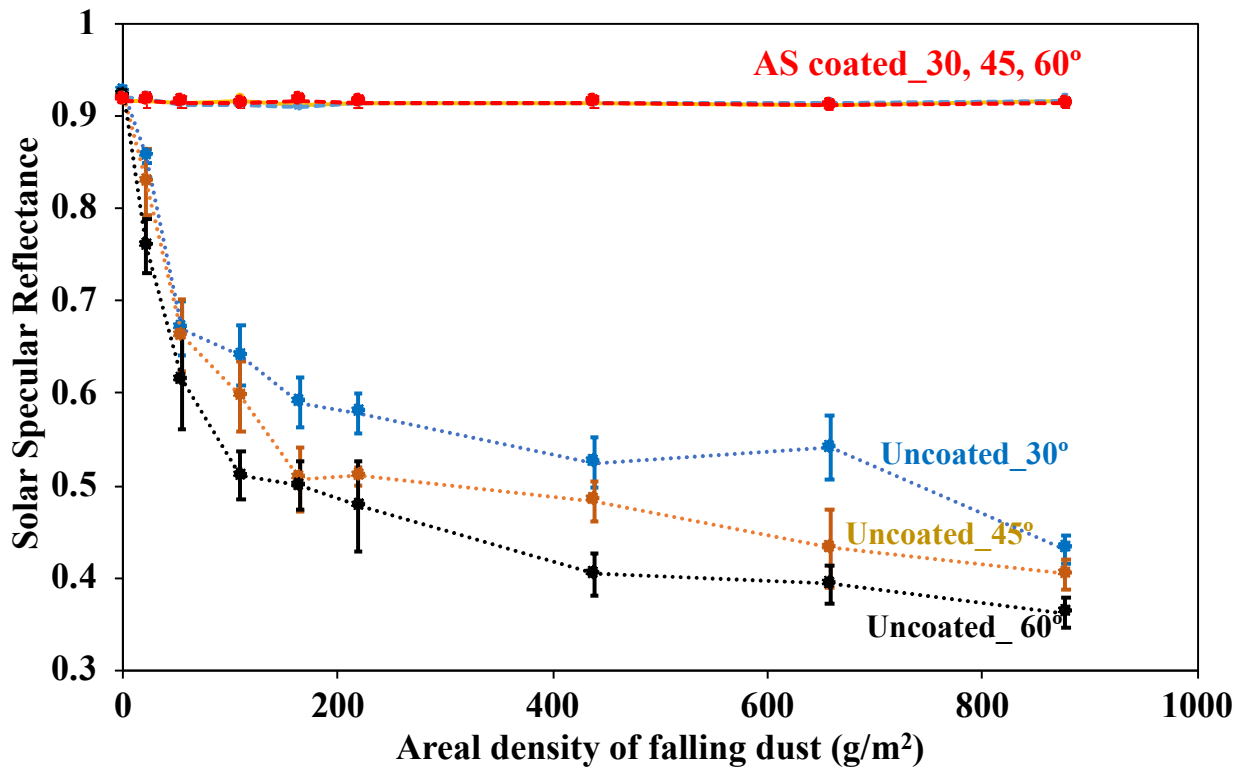

Figure 7 Changes in solar specular reflectance on AS coated mirror and uncoated mirrors as an increasing amount of dust was applied to mirrors at elevations of 30, 45 and 60° after air-brushing. The number of measurements per data point was ≥ 5, and the error bars are the standard deviations in mean values. Lines are drawn for illustration and are not modelled curve fits to the data.

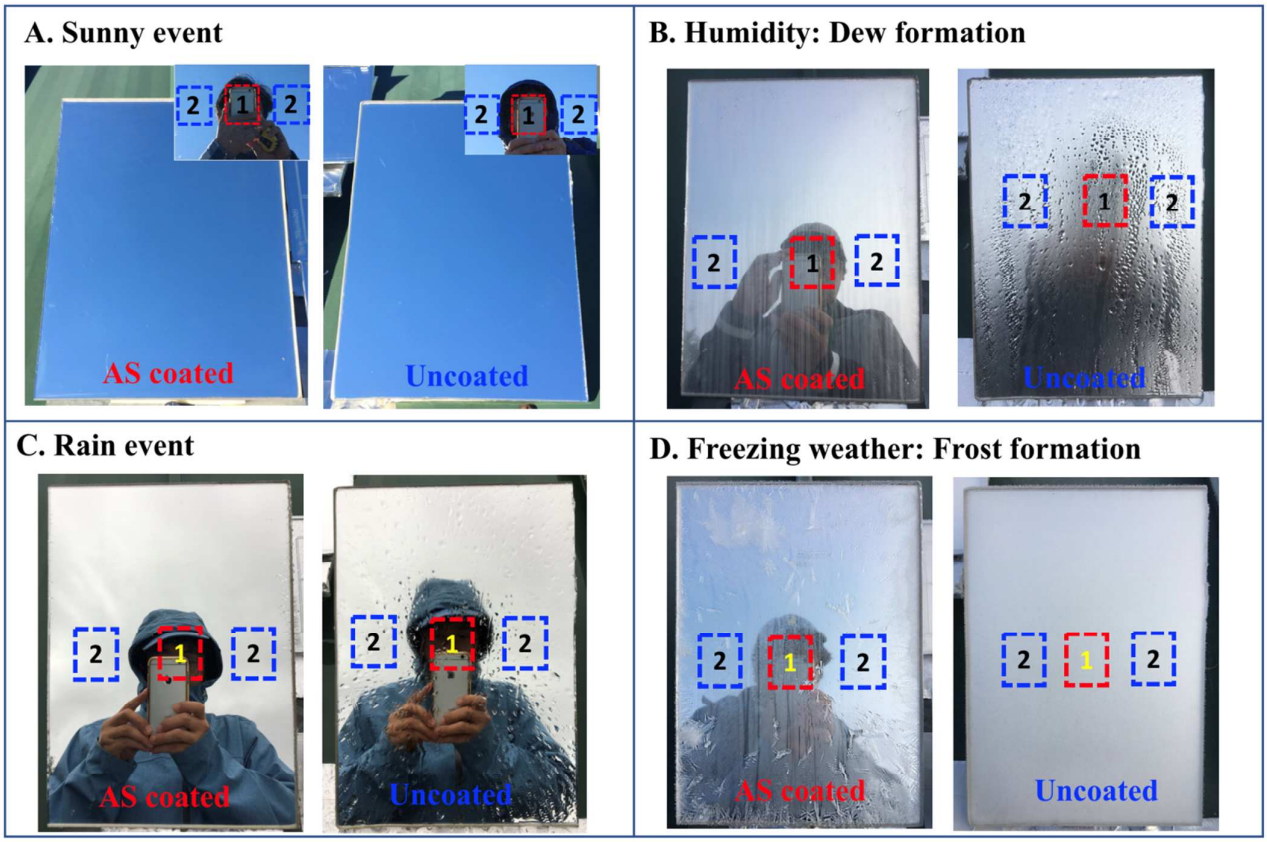

Figure 8 Observations of mirror surface conditions in a range of environmental conditions while field testing in Oak Ridge, Tennessee, USA. Appearances of the AS coated mirror and uncoated mirror for weather conditions experienced during the field test. a) Sunny condition, b) High humidity with temperature below the dew point results in condensation on mirror surfaces, c) Rain event, d) Condensation with temperature below freezing results in frost formation. Rectangular outlines indicate areas where the images were analysed to compare the luminances of the mirror surfaces.

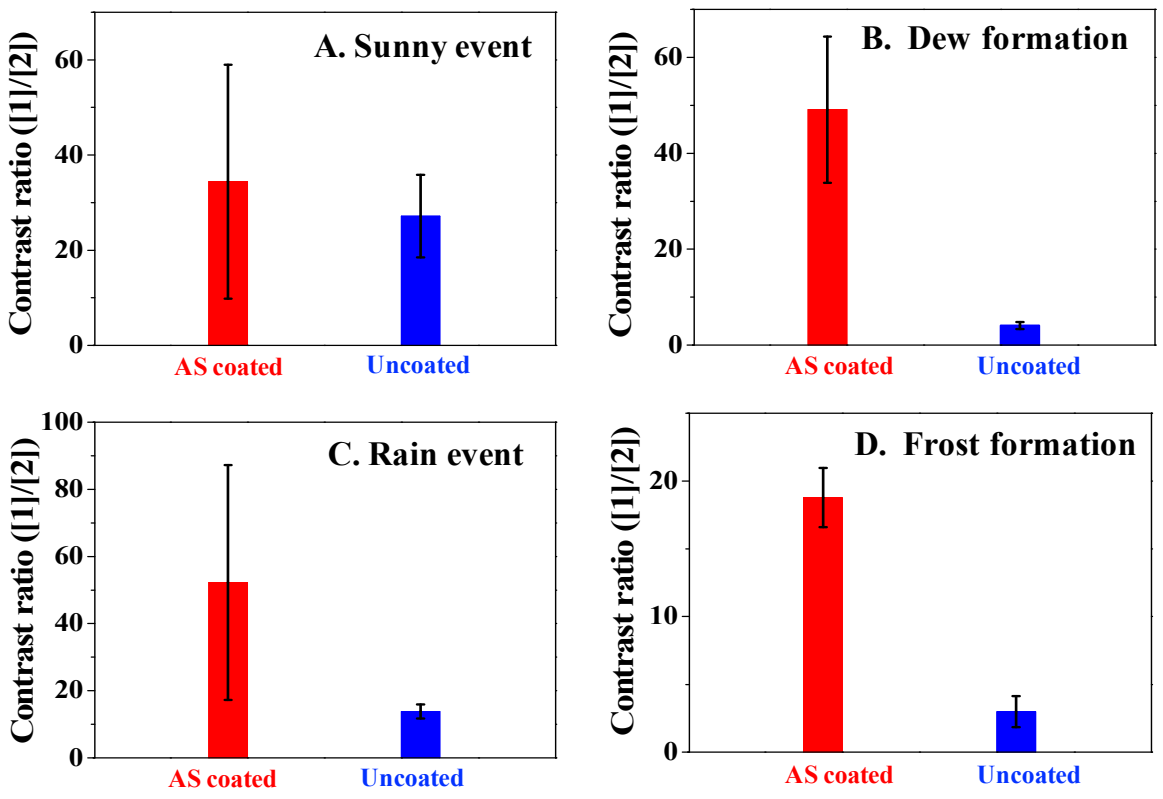

Figure 9 Contrast ratio analysis of corresponding images from AS coated mirror vs. uncoated mirror for water associated weather events in figure 8; a) Sunny event, b) Dew formation, c) Rain event, d) Frost formation

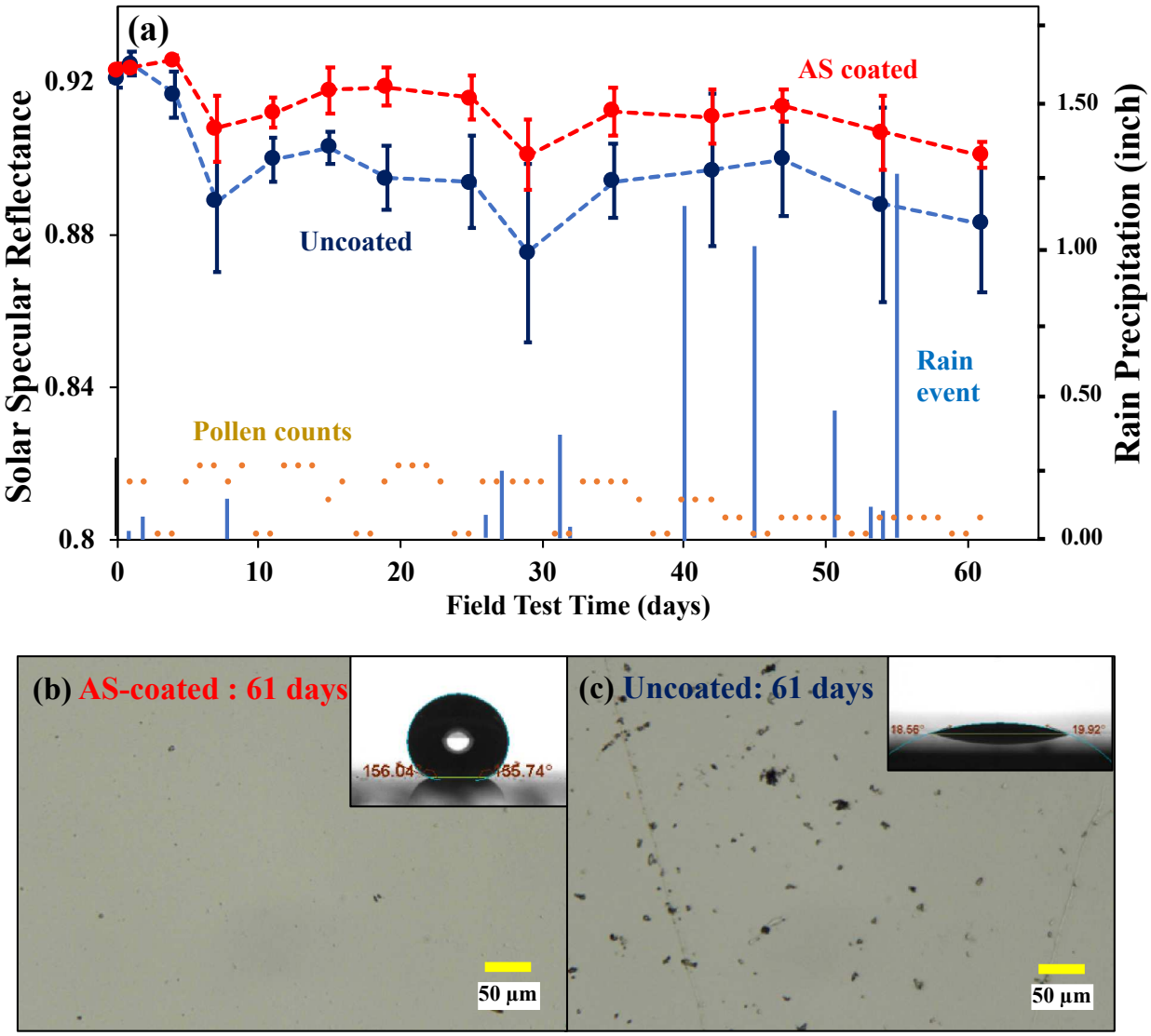

Figure 10 a) Solar specular reflectances of AS coated and uncoated mirrors measured during 61-day-long outdoor exposure. Blue bars and orange dots indicate the precipitation levels and airborne pollen counts during the field test period. The maximum pollen count was 4 grains/m^3 during the test period), b) The surface of AS coated mirror after field test, c) The surface of the uncoated mirror. The number of measurements per data point was ≥ 5, and the error bars are the standard deviations in mean values. Lines are drawn for illustration and are not modelled curve fits to the data.

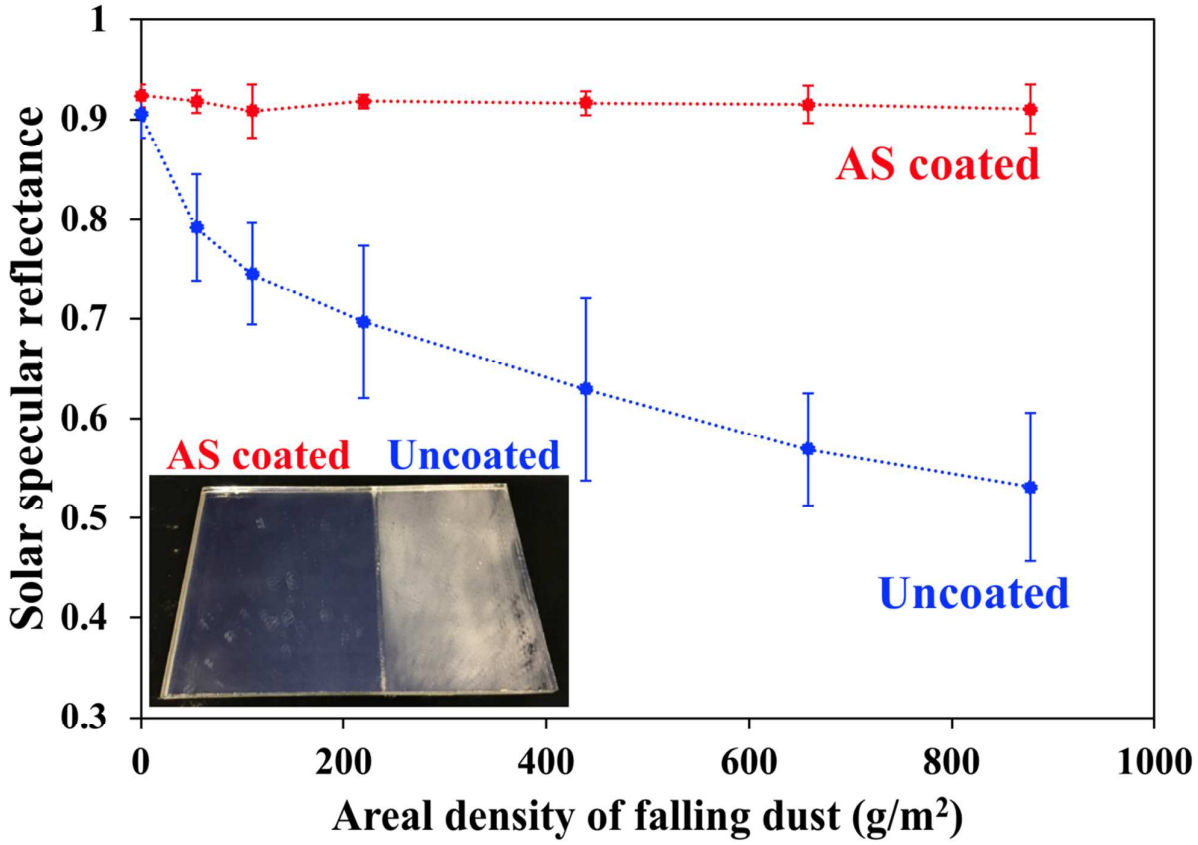

Figure 11 Specular reflectance measurements on three sample mirrors (AS coated vs. Uncoated) following applications of falling dust with mirror elevated at 45°. Mirrors were exposed to concentrated UV radiation to accelerate the dose rate in an aging procedure with cumulated dose equivalent to a one-year UV exposure in the Arizona desert. Number of measurements per data point was ≥ 15. Error bars are standard deviations in mean values of reflectance. Lines are drawn for illustration and are not fitted to data.

Table of content

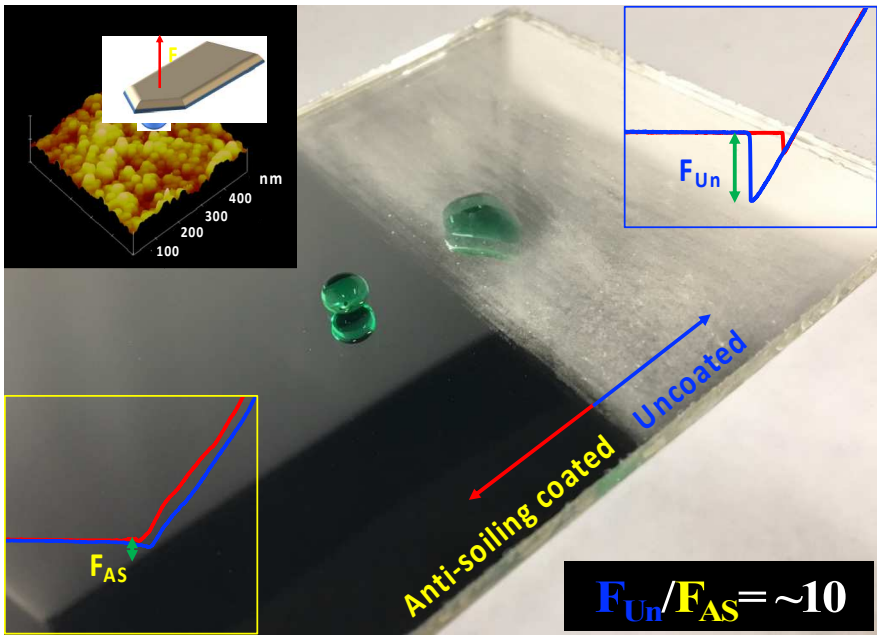

Highly transparent, superhydrophobic nanoparticle-textured coatings with engineered surface roughness significantly decrease the adhesion force of dust particles on the surface, resulting in soil and dust repellent performance.